GLOBAL BIOGEOCHEMICAL CYCLES, VOL. 12, NO. 1, PAGES 193–210, MARCH 1998

Quantification of diffusive benthic fluxes of nitrate, phosphate, and silicate in the southern Atlantic Ocean

Christian Hensen, Holger Landenberger, Matthias Zabel, and Horst D. Schulz

Department of Geosciences, University of Bremen, Bremen, Germany

Abstract. Pore water data from surface sediments and bottom water data at 180 locations were used to create distribution maps of diffusive benthic release rates of nitrate, phosphate, and silicate in the southern Atlantic Ocean for water depths ≥1000 m. Geostatistical methods of variogram analysis and kriging were used for data interpolation. Since benthic fluxes are controlled by organic matter degradation and dissolution processes and therefore by the supply of organic matter to the sediment surface, the distribution pattern of all investigated constituents should reflect a general coupling to surface water productivity. This seems to be true for the most part of the oligotrophic central South Atlantic and the upwelling area off southwest Africa. Striking regional differences in this regard, however, exist for the eastern equatorial region where unexpectedly low fluxes were calculated and the Argentine Basin where benthic fluxes are very high. The Argentine Basin obviously receives a higher input of degradable/dissolvable material, whereas in the eastern equatorial region the low benthic fluxes are possibly due to intense nutrient recycling within the water column. Estimated fluxes vary considerably over the entire region: NO_3, 10-180 mmol m^{-2} yr^{-1}; PO_4, (-2)-11 mmol m^{-2} yr^{-1}; and Si, 0-0.65 mol m^{-2} yr^{-1}. Areas of highest release rates are the continental margins off southwest Africa and off Argentina. The investigated area comprises a total of approximately 32×10^6 km^2 between 8°N and 40°-50°S. Our estimations reveal benthic release rates of 1.55×10^{12} mol NO_3 yr^{-1}, 3.5×10^{10} mol PO_4 yr^{-1} and 2.1×10^{12} mol Si yr^{-1}. Open ocean areas with middle to low fluxes contribute about 70-80% of the total estimated fluxes. The release of phosphate is probably underestimated because of core recovery artifacts and is therefore based on the assumption that fluxes are not lower than 0.25 mmol m^{-2} yr^{-1} at any location of the studied area. The investigated area represents about one tenth of the world deep ocean (without the Arctic Ocean). Assuming the South Atlantic to be representative, we calculate annual global release rates of 15×10^{12} mol NO_3, 32×10^{10} mol PO_4 and 20×10^{12} mol Si. If our estimates are correct, about 4-6% of silicate, 3-4% of nitrate, and 1% of phosphate annually produced in the surface waters are remineralized in surface sediments from water depths ≥ 1000 m.

1. Introduction

The quantification of processes controlling marine biogeochemical cycles is a major task when calculating mass balances within the oceans. A key position for global calculations concerns the cycling of carbon and nutrients in the oceans. The most important questions are as follows: (1) How much organic matter (OM) is produced/fixed in the surface waters? (2) How much OM is exported to deeper waters and the sediment surface? (3) What fraction of OM arriving the seafloor is buried and what fraction is released back into the bottom water through mineralization/dissolution processes. There are numerous publications dealing with the global oceanic primary production [e.g., *Berger et al.*, 1987, *Berger, 1989; Berger and Wefer*, 1991; *Antoine et al.*, 1996], empirical relationships for export production depending on water depth [*Suess, 1980*; *Betzer et al.*, 1984; *Berger et al.*, 1987, 1989] and the efficiency of remineralization and burial [*Henrichs and Reeburgh*, 1987; *Emerson and Hedges*, 1988; *Canfield*, 1993]. *De Baar and Suess* [1993] estimate a 90% recycling of the annual primary production (PP) within the surface waters. Only about 1% of the remaining 10% of OM which escapes as export production to the deep ocean is buried in marine sediments. The important link between burial of OM and the enhancement of PP (by nutrient reflux) in the surface waters is the biogeochemical mineralization efficiency in the deep waters and within the surface sediments. *Jahnke and Jackson* [1987] conclude from seafloor oxygen consumption rates in the North Pacific that below a water depth of 3000 m seafloor respiration is the dominant process in total deep ocean metabolism. The quantification of benthic release rates therefore plays an essential role in estimating total amounts of deep ocean mineralization.

From a global perspective it seems to be possible to estimate the rain of biogenic debris to the seafloor (and therefore the benthic activity) from PP and the depth dependence from empirical relationships of OM export (i.e., derived from sediment traps). On a regional scale, however, this is subject to substantial uncertainties because there are significant differences in predictions of primary productivity in certain areas [cf. *Berger and Wefer*, 1991; *Antoine et al.*, 1996] and lateral input of OM to the sediment, especially along continental margins [*Jahnke et al.*, 1990; *Rowe et al.*, 1994]. Recently, *Jahnke* [1996] investigated benthic

Paper number 97GB02731.
0886-6236/98/97GB-02731$12.00

oxygen fluxes and calculated equivalent fluxes of particulate OM to the seafloor on a global scale. Since direct flux measurements are of restricted availability, the estimations were based on empirical correlations between measured fluxes and sediment parameters (organic carbon and calcium carbonate contents and accumulation rate). It is difficult to assess to what extent these estimations can be used for predictions of the benthic refluxes of nutrients, which are released during OM degradation, such as phosphate and nitrate. The released amounts of nitrate and phosphate strongly depend on the C:N:P ratio of the OM mineralized. Furthermore, adsorption on solid phase surfaces (phosphate), denitrification, and ammonium oxidation may play important roles in influencing the amounts of nitrate and phosphate released from sediments. Similiar problems exist for the derivation of benthic silicate fluxes from surface water opal production or opal rain rates. *Archer et al.* [1993] found a correlation between opal rain rate and diffusive silicate flux, but claimed a general lack of understanding in the diagenesis of opal.

In our study we applied an approach to estimate benthic release rates for a larger oceanic area similiar to those of *Zabel et al.* [1997]. Owing to the uncertainties resulting from empirical correlations and a general lack of information on nutrient release from the deep ocean sediments, we used our pore water data set obtained over several years to produce distribution maps of nitrate, phosphate, and silicate for the southern Atlantic Ocean between 8°N and 40-50°S. A total of about 180 locations (including literature data) permitted analysis with geostatistical interpolation methods. We present estimations for totally released amounts of nitrate, phosphate, and silicate, mean release rates, and regional variations of the nutrients in the South Atlantic as well as global projections.

2. Study Area and Locations

Pore and bottom water samples were collected during seven expeditions of FS Meteor in the southern Atlantic Ocean from 1988 to 1996 (Table 1). All sampling locations are listed in Table 2 including water depth and are illustrated in Plate 1. Additional pore water data for the equatorial region from *Froelich et al.* [1979] and *Jahnke et al.* [1989] are included. Most of the locations are clustered on transects along the continental margins of South America and southwest Africa, where the highest benthic activity was expected from PP maps. Proportionally few transects cover the large central basin and Mid-Atlantic ridge area, where variability was expected to be low. In summary, the investigated area covers a considerable part of the South Atlantic with large-scale variations in the oceanic and sedimentary setting, which are caused by differences of surface and subsurface water currents, regional wind systems, bio-productivity, terrigenous sediment input, and basin morphology.

3. Methods

3.1. Sampling and Geochemical Analyses

Surface sediments were retrieved by box corer and/or mostly multicorer sampling. To reestablish in situ temperatures on board the ship, after a transient heating during recovery through the water column, the sediments were immediately stored in a cooling laboratory at approximately 4°C. After careful removal of the bottom water by siphoning the cores were cut into slices as thin as 0.5 cm near the sediment surface to achieve the highest possible depth resolution there. Pore water was extracted using a cooled centrifuge (M20-2, Table 1) or teflon squeezers (all additional cruises) with 0.2 μm membrane filters. Results of both procedures were shown to be in good agreement [*Jahnke et al.*, 1982a; *Schulz et al.*, 1994]. However, results of *Berelson et al.* [1990] and *Hammond et al.* [1996] show increased subsurface peaks of nitrate in centrifuged samples which is discussed in section 3.3.

Phosphate and nitrate (nitrate plus nitrite) were analyzed within a few hours after recovery. The remaining pore water was acidified with HNO_3 (65%) and stored at 4°C until further analysis at the University of Bremen. Bottom and pore water concentrations of nitrate and phosphate were determined with

Table 1. Cruise and Core Numbers, Dates, and Sampling Areas

Cruise	GeoB	Month and Year	Area
M6-6	10..	February/March 1988	West Africa/equatorial
M9-4	11..	February/March 1989	equatorial
M16-1	14..	April 1991	equatorial/central
M16-2	15..	May 1991	central/equatorial
M20-2	17..	January 1992	West Africa
M23-1	20..	February 1993	West Africa/central
M23-2	21..	March 1993	central
M23-3	22..	March/April 1993	equatorial
M29-1	27..	June/July 1994	Argentina
M29-2	28..	July 1994	Argentina/central
M29-3	29..	August 1994	central/equatorial
M34-1	36..	January 1996	SW Africa
M34-2	37..	January/February 1996	SW Africa
M34-3	38..	February/March 1996	central
M34-4	39..	March/April 1996	equatorial
Jahnke et al. [1989]		November 1987	equatorial
Froelich et al. [1979]		May 1976	equatorial

GeoB means Geoscience Bremen stations. Numbers with double periods indicate all GeoB stations beginning with the specific number.

Table 2. Sampling Locations, Water Depth, and Diffusive Benthic Fluxes

Station GeoB	Longitude,[a] deg	Latitude,[b] deg	Water Depth, m	Nitrate, mmol $m^{-2}yr^{-1}$	Phosphate, mmol $m^{-2}yr^{-1}$	Silicate, mol $m^{-2}yr^{-1}$
1008	10.32	-6.59	3100	-	0.60 [c]	0.11 [c]
1015	12.84	-11.78	1650	-	0.12	-
1018	8.89	-11.73	4530	10	0.13 [c]	0.06 [c]
1023	11.00	-17.16	1855	-	-	0.15 [c]
1028	9.19	-20.10	2215	-	1.05 [c]	0.07
1031	7.10	-21.88	3103	11	0.18	0.04
1035	5.02	-21.58	4450	6	0.24 [c]	0.01
1037	0.15	-13.15	5626	32 [c]	-0.33 [c]	0.02 [c]
1041	-7.60	-3.47	4035	26 [c]	0.19 [c]	0.02
1043	-9.91	-0.01	5159	34 [c]	0.10	0.03
1101	-10.98	1.67	4567	15 [c]	-0.09 [c]	0.03 [c]
1104	-10.73	-1.16	3724	10	0.16 [c]	0.06
1111	-8.65	-5.84	3757	12 [c]	0.22 [c]	0.02 [c]
1117	-14.72	-3.81	3977	9	0.31	0.04
1401	9.01	-6.93	3949	-	0.00	0.10
1403	-11.71	-1.20	3692	33	0.06	0.08 [c]
1404	-10.78	-0.08	3988	38	-	-
1405	-11.14	1.79	4354	29	0.06	0.06
1406	-11.24	3.16	4523	34	-	-
1407	-10.25	-4.32	3504	54	-0.31	0.07
1412	-7.76	-15.67	4342	5	-	-
1413	-9.46	-15.68	3785	36	-0.40	0.01
1420	-18.69	-15.36	4587	-	-0.61 [c]	0.01 [c]
1421	-24.76	-12.85	5045	4 [c]	-	-
1501	-32.01	-3.68	4258	7	-0.12	0.03
1505	-33.02	2.27	3703	11	0.27 [c]	0.06
1508	-34.03	5.33	3681	35	0.42 [c]	0.10
1511	-46.34	3.18	3162	-	0.75	0.04
1512	-48.04	5.90	3718	20	2.42 [c]	0.12
1514	-46.58	5.14	3511	27	0.70 [c]	0.06
1701	3.55	1.95	4162	40	0.24	0.09
1702	10.32	-6.57	3094	109	1.28	0.21
1703	11.02	-17.45	1771	-	6.93	0.45
1704	11.61	-19.41	395	-	4.21	0.13
1706	11.18	-19.56	980	-	2.54 [c]	0.53 [c]
1708	8.96	-20.09	2321	126	2.55	0.10
1710	11.70	-23.43	2988	-	1.38	0.07 [c]
1711	12.37	-23.32	1982	90	2.22	0.15
1712	12.81	-23.25	1004	-	8.70	0.18
1713	13.01	-23.22	600	-	14.95	0.34
1715	11.64	-26.47	4095	46	0.35	0.16
1716	14.00	-27.95	1485	122	1.80	0.09
1719	14.17	-28.93	1023	153	2.26	0.06
1720	13.84	-29.00	2004	164	1.53	0.07
1721	13.09	-29.17	3045	144	0.60	0.04
1722	11.75	-29.45	3974	118	-0.52	0.04
1724	8.04	-29.97	5102	22	-0.68	0.03
1726	3.27	-30.27	1007	16	-	-
1729	1.00	-28.89	4401	16	0.12	0.05
2002	15.48	-31.49	1043	218	7.29	0.20
2004	14.35	-30.87	2571	268	4.15	0.16
2010	10.29	-32.86	5049	-	-0.19 [c]	0.01 [c]
2011	8.27	-35.58	5067	-	-0.40 [c]	0.03 [c]
2016	-1.30	-31.91	3385	29	-2.06	0.04
2018	-6.55	-34.67	4237	103	-1.11	0.03
2019	-8.77	-36.05	3836	85	1.50	0.08
2021	-14.41	-36.84	3576	61	0.52	0.05
2022	-20.92	-34.43	4016	69	0.00	0.04
2102	-41.20	-23.98	1805	10	4.33	0.03
2104	-46.38	-27.29	1505	124	2.80	0.04
2105	-46.74	-26.74	202	52	0.96	0.03
2106	-46.50	-27.10	502	96	3.35	0.04
2107	-46.45	-27.18	1045	41	3.28	0.08
2108	-46.23	-27.49	1991	88	2.83	0.01
2110	-45.52	-28.65	3003	118	-1.99	0.08
2112	-43.38	-29.14	4009	112	1.00	0.04
2116	-36.00	-25.51	4164	17 [c]	-1.99	0.01

Table 2. (continued)

Station GeoB	Longitude,[a] deg	Latitude,[b] deg	Water Depth, m	Nitrate, mmol $m^{-2}yr^{-1}$	Phosphate, mmol $m^{-2}yr^{-1}$	Silicate, mol $m^{-2}yr^{-1}$
2117	-36.65	-23.04	4047	169	0.77	0.22
2118	-38.02	-22.09	3482	57	0.63	0.00
2119	-38.55	-21.73	2958	28	1.05	0.05
2124	-39.56	-20.96	2003	51	0.26	0.01
2125	-39.86	-20.82	1542	-	5.84	0.09
2126	-38.93	-21.27	2537	111	2.58	0.03
2201	-34.46	-8.17	794	85	4.17	0.19
2202	-34.26	-8.21	1128	-	3.51	0.08
2204	-34.02	-8.53	2080	72	1.73	0.11
2205	-34.35	-8.58	1790	121	0.00	0.01
2208	-33.70	-8.93	3977	34	-0.61	0.05
2212	-25.62	-4.03	5521	244	2.12	0.05
2213	-24.15	-1.27	4323	96	3.42	0.12
2215	-23.49	0.00	3712	76	5.94	0.05
2216	-23.10	0.00	3914	-	2.28	0.05
2703	-54.20	-38.51	1162	-	4.21	-
2704	-53.93	-38.93	3247	249	11.02	0.30
2705	-53.36	-39.24	4474	-	11.02	0.63
2706	-55.54	-42.37	4700	151	9.00	0.16
2707	-56.32	-41.95	3167	246	4.30	0.27
2708	-57.30	-41.42	392	56	8.14	-
2709	-57.06	-41.54	1080	-	4.62	0.09
2712	-59.33	-43.67	1230	65	5.59	0.01
2714	-58.00	-43.86	2361	286	5.83	0.51
2715	-57.66	-43.90	3280	225	3.98	0.41
2717	-56.49	-47.16	4479	184	11.48	0.73
2718	-58.18	-47.31	2990	114	1.16	0.10
2719	-60.09	-47.44	684	62	6.37	0.42
2722	-58.62	-47.33	2351	242	7.32	0.64
2723	-57.88	-48.91	569	40	4.68	0.09
2724	-56.18	-47.96	4799	143	6.21	1.13
2726	-56.93	-48.39	1405	85	0.71	0.02
2727	-56.54	-48.01	2803	113	1.40	0.19
2729	-56.98	-44.00	4700	162	6.37	0.39
2730	-53.25	-44.48	5845	136	4.73	0.25
2731	-51.42	-44.21	5697	155	7.69	0.42
2801	-54.17	-37.04	490	81	4.23	0.18
2802	-53.97	-37.20	1007	71	3.98	0.19
2803	-53.70	-37.41	1162	-	7.06	0.36
2804	-53.54	-37.54	1836	270	13.60	0.47
2805	-53.44	-37.61	2743	228	18.92	0.38
2806	-53.14	-37.83	3542	187	15.33	0.58
2807	-52.32	-38.47	4481	150	5.42	0.51
2808	-50.63	-37.01	4541	128	4.27	0.38
2809	-51.52	-36.33	3539	276	16.56	0.37
2810	-51.98	-35.98	2909	286	14.20	0.26
2811	-52.27	-35.75	1789	-	20.01	0.40
2812	-52.39	-35.60	1041	29	2.73	0.40
2813	-52.56	-35.53	511	63	1.60	0.19
2814	-39.07	-37.60	4949	68	2.57	0.07
2817	-38.07	-30.92	2943	47	0.58	0.04
2818	-38.17	-30.87	3110	37	0.68	0.02
2820	-38.44	-30.82	3606	63	0.01	0.02
2824	-42.50	-33.50	4512	-	4.65	0.36
2825	-41.43	-32.51	4352	96	-0.67	0.19
2826	-40.97	-31.90	3959	176	3.27	0.12
2828	-40.72	-31.48	3741	-	-	0.33
2829	-43.43	-30.87	3523	183	-1.10	0.02
2903	-28.03	-7.55	5637	63	-	-
2904	-25.66	-4.06	5579	190	0.02	0.41
2905	-28.64	-0.66	4166	134	0.54	0.13
2906	-27.25	-0.41	3870	121	0.31	0.14
2907	-25.51	-0.43	3675	95	0.63	0.06
2908	-23.32	0.11	3815	230	0.21	0.18
2909	-21.63	0.50	4383	112	0.44	0.04
2910	-21.05	4.85	2701	233	0.89	0.04
3608	12.20	-22.36	1973	-	23.38	0.49
3701	14.01	-27.95	1488	-	9.47	0.11

Table 2. (continued)

Station GeoB	Longitude,[a] deg	Latitude,[b] deg	Water Depth, m	Nitrate, mmol $m^{-2}yr^{-1}$	Phosphate, mmol $m^{-2}yr^{-1}$	Silicate, mol $m^{-2}yr^{-1}$
3702	13.46	-26.79	1319	65	3.09	0.96
3703	13.23	-25.52	1376	136	15.73	0.88
3704	13.08	-25.47	1780	142	16.94	0.73
3705	13.00	-24.30	1305	61	10.80	0.66
3706	12.60	-22.72	1313	140	4.12	0.42
3707	12.19	-21.63	1350	161	15.54	0.75
3713	11.58	-15.63	1330	136	-	0.26
3714	11.00	-17.16	2060	232	13.84	1.27
3715	11.06	-18.96	1204	206	11.08	0.43
3717	13.35	-24.83	855	229	14.33	0.89
3718	13.16	-24.90	1316	139	5.98	0.87
3719	12.87	-25.00	1995	202	-	0.56
3721	12.40	-25.15	3014	138	3.32	0.54
3724	8.93	-26.14	4763	36	-2.28	0.24
3801	-8.30	-29.51	4534	22	0.07	-
3802	-8.52	-30.16	3970	73	0.56	0.14
3803	-8.72	-30.35	4173	37	0.08	0.09
3804	-8.77	-30.74	3882	91	0.07	0.11
3808	-14.71	-30.81	3213	13	-2.47	0.05
3809	-16.33	-31.05	3470	51	-	0.16
3810	-16.84	-31.13	3810	41	-2.98	0.00
3812	-19.76	-31.62	4204	49	-2.37	0.12
3822	-37.95	-27.63	4273	34	-0.75	0.05
3825	-36.33	-26.23	4279	57	1.75	0.23
3827	-38.55	-25.03	3842	33	-1.27	0.09
3906	-28.11	-7.47	4886	12	0.07	0.00
3908	-23.43	-0.01	3693	39	0.21	0.04
3909	-36.27	-3.55	3174	74	0.00	0.04
3910	-36.35	-4.25	2361	63	0.41	0.03
3911	-36.64	-4.61	826	206	2.05	0.09
3914	-38.23	-2.73	2461	50	-	0.02
3915	-38.02	-2.28	3127	161	0.08	0.09
3925	-47.53	5.14	3198	134	1.14	0.14
J8	-20.47	4.96	2760	62	0.69	0.16
J10	-19.67	2.13	5036	20	-0.30	0.06
J11	-22.78	1.96	4210	-	1.55	0.06
J11.5	-22.89	0.94	4419	29	0.20	0.07
J12	-23.00	0.01	3858	-	2.15	0.07
J12.5	-23.00	-1.01	4630	48	5.51	0.10
J13	-23.01	-2.11	4950	-	3.00	0.05
J14	-23.00	-4.97	5102	-	0.27	0.04
J15	-22.97	-7.97	5358	-	-1.60	0.04
F24	-9.07	0.03	4572	-	0.16	-
F23	-10.56	0.07	4901	-	0.10	-
F11	-12.32	-0.00	4980	-	0.13	-
F12	-8.21	1.10	3880	-	0.20	-
F14	-6.68	2.85	4170	-	0.07	-

Dash indicates data not available. Stations J8-J15 and F11-F14, F23, and F24 are calculated according to data from *Jahnke et al.* [1989] and *Froelich et al.* [1979], respectively.

[a] Negative longitude indicates west.

[b] Negative latitude indicates south.

[c] Fluxes calculated (or corrected) with bottom water concentrations taken from the Geochemical Ocean Sections Study [*Bainbridge*, 1976].

autoanalyzers using standard photometrical procedures described by *Grasshoff et al.* [1983]. Silicon was analyzed with a plasma emission spectrometer (Perkin-Elmer ICP/6500 XR). For more detailed description of sediment sampling and chemical analysis, see *Schulz et al.* [1994].

3.2. Calculation of Benthic Fluxes

Benthic fluxes were calculated using Fick's first law of diffusion (Equation (1)) assuming steady state conditions.

$$J = -\phi \times D_s \times \frac{\partial C}{\partial x} \quad (1)$$

where J is the diffusive flux, D_s is the molecular diffusion coefficient in the sediment, ϕ is the porosity, and $\partial C/\partial x$ is the concentration gradient. Molecular diffusion coefficients of the investigated species were taken from *Li and Gregory* [1974], *Lerman* [1979] and *Rutgers van der Loeff*, and *van Bennekom* [1989] and recalculated with regard to changes of viscosity for 4°C (Table 3). Considering tortuosity, diffusion coefficients in the sediment

Table 3. Molecular Diffusion Coefficients in Water

	Si, $m^2\ yr^{-1}$	HPO_4^{2-}, $m^2\ yr^{-1}$	NO_3^-, $m^2\ yr^{-1}$
Diffusion coefficient (literature data)	0.0145 [a]	0.0231 [b]	0.0308 [c]
Diffusion coefficient (4°C)	0.0167	0.0134	0.0356

[a] 0°C [*Rutgers van der Loeff and van Bennekom*, 1989]
[b] 25°C [*Li and Gregory*, 1974]
[c] 0°C [*Lerman*, 1979]

were calculated with the empirical equation of *Ullman and Aller* [1982, Equation (2)]

$$D_s = \phi^{(n-1)} \times D_m \quad (2)$$

where D_m is the molecular diffusion coefficient in water, and n is a correction factor (n=3, if porosity ≥0.7; n=2, if porosity < 0.7). Porosity was calculated from dry bulk density (P.J. Müller, unpublished data, 1989-1992) or from conductivity measurements on a parallel multicorer core. Generally, a porosity of 0.85-0.95 can be presumed as a mean for the uppermost 0-0.5 cm interval. The concentration gradient ($\partial C/\partial x$) was determined by a two-point calculation between the concentration in the uppermost interval and the bottom water concentration, assuming that bottom water concentrations do not fluctuate considerably close to the interface. At some locations (footnoted values in Table 2), bottom water values were assigned using data from *Bainbridge* [1976]. Effects on benthic fluxes due to the existence of a diffusive sublayer were not considered.

3.3. Limitations of Flux Calculations

Calculation of benthic fluxes according to the method described above is subject to uncertainties which need to be considered as follows. All calculations were made under the premise that vertical diffusion is the exclusive transport mechanism. The dominance of diffusive transport was recently demonstrated by *Sayles and Martin* [1995] at least for oligotrophic ocean conditions. This may, however, lead to significant errors along the continental margins, where macrobenthic irrigation becomes more important because of higher input of OM [*Aller*, 1988; *Glud et al.*, 1994]. A general dependence on water depth is not observed [*Glud et al.*, 1994], but most striking differences between total and diffusive fluxes exist on continental shelves [*Archer and Devol*, 1992]. Therefore, as an operative approach to reduce this error, our predictions exclude areas with water depths shallower than 1000 m. Furthermore, the number of stations from shallower water depths is very low (10) and therefore seems to be insufficient for extrapolation. Flux calculations from those stations are only used for data (trend) interpolation between 1000 m water depth and deeper.

It can be inferred from Table 1 that the cruises cover most of the seasons. This helped to reduce possible effects of seasonality in certain areas (central equatorial Atlantic). However, in the major part of the study area, flux measurements are the results from single cruises or from several cruises to the same region carried out during the same season. For this reason we are not able to exclude seasonal effects of PP and export of OM on the benthic activity as described by *Smith and Baldwin* [1984]. However, *Sayles et al.* [1994] argue that large areas of the seafloor undergo very limited temporal variation in metabolic rates. In section 4.1. we show for a limited region that seasonality could be the more important factor controlling benthic activity at the sediment surface, the general flux pattern, however, we believe is not basically affected by seasonal variations.

A further point that should be kept in mind are effects due to core recovery and processing. As already described by *Jahnke et al.* [1982a], the degassing of CO_2 and the resulting precipitation of $CaCO_3$ also affects pore water concentrations of phosphate (adsorption and coprecipitation). *Zabel et al.* [1997] report a decrease of up to 1 μmol $PO_4^{3-}\ L^{-1}$ in surface sediments compared to unaffected bottom water concentrations in areas with low phosphate release rates. This effect can imply negative fluxes (Table 2) as noted in the discussion below.

Transient heating of a core leads to enhanced microbial activity and oxygen consumption [*Glud et al.*, 1994] and might also lead to elevated pore water concentrations of nitrate. *Hensen et al.* [1997] demonstrated for GeoB (Geoscience Bremen) 1702 and 1711 that benthic oxygen fluxes were not sufficient to create high subsurface nitrate concentrations (under the assumption that degradable OM has C/N molar ratio of 6.6 and organic nitrogen is completely oxidized to nitrate). A lower C/N ratio of degraded OM or an oxidation of more favorable nitrogen compounds (e.g., ammomium) would be suitable explanations of increased nitrate fluxes. However, *Hammond et al.* [1996] identified increased subsurface nitrate peaks to be apparently an artifact of centrifugation. Squeezing and centrifugation techniques were not performed at the same stations so that it is difficult to evaluate inherent differences. However, the analysis of nitrate fluxes calculated from pore water results obtained by both methods in one geographical area (continental margin off Namibia) do not show significant trends (Table 4). In contrast, *Jahnke et al.* [1982a, 1989] did not report significant deviations between in situ and laboratory pore water concentrations of nitrate. Recent comparisons of nitrate fluxes obtained from benthic chamber measurements and whole core squeeezer methods in the equatorial Pacific [*Hammond et al.*, 1996] indicate reasonably good agreement between these two methods, but the result is difficult to transfer to the applied squeezing method. Since artificially increased nitrate subsurface concentrations due to core retrieval and/or pore water extraction are probable, the nitrate fluxes are interpreted as maximum estimates.

The calculation of fluxes from linear gradients might, however, introduce uncertainties since pore water profiles often (especially silicate) display an asymptotic curvature to the sediment surface. For a depth resolution of mostly ≤ 1cm we assume this effect to be neglible relative to the above factors. As an example calculation for a nonlinear approximation, we fitted silicate pore water profiles to an exponential function (Equation (3)) as given by *Sayles et al.* [1996]:

$$[SiO_2] = a_1 + a_2 \times \left(1 - \exp(a_3 \times x)\right) \quad (3)$$

where a_1 is the bottom water concentration; a_2 is the difference between maximum pore water concentration and bottom water concentration; a_3 is the depth attenuation coefficient; and $a_2(-a_3)$ is the first derivative at depth x=0. The fluxes derived from the asymptotic fit function agree fairly well (14% and 15% deviation,

Table 4. Comparison of Nitrate Fluxes Off Southwest Africa Obtained by Different Extraction Methods

Method	Number of Stations	Mean Nitrate Flux	Minimum Nitrate Flux	Maximum Nitrate Flux
Centrifugation	(4)	132 (± 33)	90	164
Squeezing	(9)	142 (± 55)	61	221

The stations are from the continental slope between 1000 and 2000 m water depth obtained by centrifugation (M 20/2) and squeezing (M 34/2) techniques. Fluxes are in mmol m^{-2} yr^{-1}. In parenthesis are the number of data points included and the standard deviation of the mean nitrate fluxes.

respectively). It should be mentioned that the gradient at the sediment surface depends strongly on the choice of a_3. However, determining which of the two methods describes the flux across the sediment water interface more realistic would require a more detailed data analysis that shall not be the subject of the present study.

3.4. Geostatistical Methods

Variogram analysis and ordinary kriging were used to describe regional dependencies of fluxes and for the data interpolation. For descriptions of the mathematical background the reader is referred to standard textbooks of geostatistical data analysis (e.g., *Davis*, 1986; *Akin and Siemes*, 1988; *Swan and Sandilands*, 1995). The calculations were carried out with the computer softwares GEO-EAS 1.1 [*Englund and Sparks*, 1988] and SURFER (Golden Software, Inc.,V6.03, 1996).

Geostatistical regionalization is based on the spatial analysis of a variable to be investigated, in this case fluxes, to make predictions for unexamined or sparsely sampled areas. The concept of kriging follows the determination of weighted means. The weighting of estimates is derived from a mathematical function describing the spatial structure of the variable ((semi) variogram analysis). The basic assumption of variogram analysis is that the variance of adjacent points representing a variable increases with increasing spatial separation. If the variable is subject to a spatial structure the variances increase up to a "sill" value, where they begin to scatter (see section 4.2.). The "sill" value determines the maximum distance range of the spatial dependency of the variable. Variances are calculated from comparison of all measured values for a given increment. The increment means the distance-interval, which determines the number of data-point pairs compared for the calculation of the variances. The resulting experimental variogram can be described by a mathematical function or "model variogram" (see section 4.2.), which is utilized for the subsequent weighting within the kriging procedure. Frequently, the model variogram does not intercept the origin, which means that comparatively high variances exist even within very short distances that are not resolvable within the given increment. A non zero intercept is called "nugget effect", and its cause can be inherent in small-scale variablility of physical or biological factors in closely sampled areas.

The results of the ordinary kriging analyses are displayed on homogeneous grids. They are derived from the comparison of measured values in certain distance intervals based on a weighting process given by the variogram analysis. To produce high-resolution maps, we used a single grid point distance of 1°. Every estimate results from a comparison of a certain number of measured values within the range given through the variogram. For the estimation of each grid point we included a minimum of at least three data points into the calculation to avoid an overrating of single measurements.

Kriging is usually applied to problems in mining and hydrogeology, where the Earth's curvature normally does not need to be taken into account. For the sake of the correct spatial dependencies we recalculated the location coordinates to equal-area *xy* coordinates before variogram analysis and kriging were carried out. The 90×70 matrices underlying the resulting distribution maps were transformed afterwards to produce usual *xy* plots.

4. Results and Discussion

4.1. Fluxes of Nitrate, Phosphate, and Silicate

Diffusive benthic fluxes of nitrate, phosphate, and silicate were calculated according to the method described above. Calculated fluxes and those derived from the literature [*Froelich et al.*, 1979; *Jahnke et al.*, 1989] are shown in Table 2. Because of the extensive data set, only some selected pore water profiles characterizing areas with low and high fluxes are displayed in Figure 1. Highest fluxes for all parameters were measured along the continental margins off southwest Africa and Argentina. Generally, pore water concentrations of all constituents increase from bottom water into the sediment because of OM degradation and dissolution processes.

Under open ocean conditions, nitrate is used as electron acceptor to only a low extent and therefore shows no significant gradient changes with increasing sediment depth, whereas it is diminished within a few centimeters in regions with higher OM input. As it was shown by computer simulations of nitrate pore water profiles [e.g., *Jahnke et al.*, 1982b; *Hensen et al.*, 1997], the intensity of denitrification has a significant effect on the level and the depth location of the nitrate maximum within the sediment. This must affect the amount of nitrate released into the bottom water. It is therefore not surprising that similiar nitrate fluxes can occur in both eutrophic and oligotrophic areas as long as OM supply is not the limiting parameter for oxic respiration and nitrification (without initializing significant denitrification) in open ocean settings. The complete oxidation of degradable OM at the sediment surface producing significant amounts of subsurface nitrate in open ocean areas might, however, depend on seasonal events and time constants for the degradation.

Under open ocean conditions, phosphate profiles generally display only small increases in concentration with sediment depth. Generally, pore water concentrations in these regions do not exceed 5 μmol L^{-1}, whereas off southwest Africa subsurface

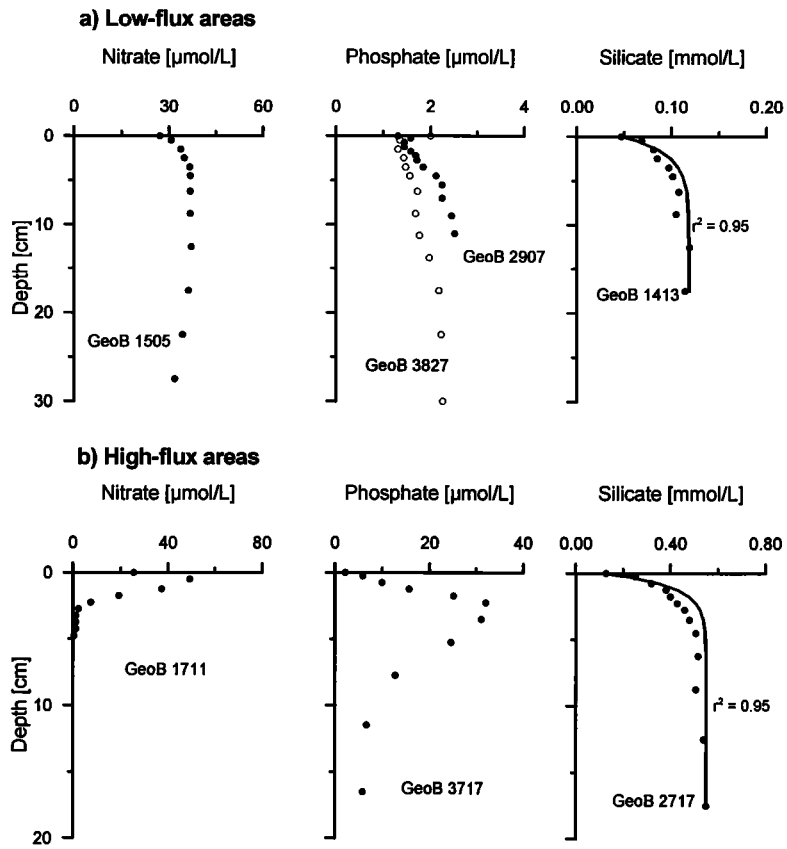

Figure 1. Typical pore water profiles of nitrate, phosphate, and silicate from various stations characterizing (a) low- and (b) high-flux areas. Silicate profiles are exemplary fitted by exponential functions as given in the text.

concentrations might exceed 20-30 µmol L^{-1}. Negative fluxes up to -3 mmol m^{-2} yr^{-1} were calculated at several open ocean locations, which are attributed to sampling artifacts (see section 3.3.). If these fluxes were true, a significant subsurface accumulation of phosphate should be detectable. For the central Atlantic we calculated a potential phosphorus concentration between 0.4 and 2.3 wt % in surface sediments, if fluxes between -0.5 and -3 mmol m^{-2} yr^{-1} (sedimentation rate is 1cm 1000 yr^{-1}; density is 2.65 g cm^{-3}; ϕ is 0.85) would be realistic. This calculated phosphorus content tends to be 1-2 orders of magnitude higher than that measured in surface sediments (e.g., GeoB 1037 is 0.07 wt %; GeoB 1413 is 0.05 wt %; and GeoB 1420 is 0.02 wt %). Therefore we conclude that negative fluxes are not realistic. While the magnitude of the decompression artifact may stay the same at all sites, the change in the near-surface gradient due to this effect decreases as the pore water phosphorus concentration increases. Therefore it becomes less significant with increasing subsurface phosphate concentrations. For this reason the general distribution pattern should not be seriously affected.

The shape of the pore water concentration profiles of silicate does not show remarkable differences between high- and low-flux areas. Maximum subsurface pore water concentrations vary between 0.1 and >0.4 mmol L^{-1} from low- to high-flux areas.

However, overall fluxes of all constituents vary by about 2 orders of magnitude, emphasizing the great heterogeneity within the studied area. Flux variability ranges from 4 to 285 mmol m^{-2} yr^{-1} for nitrate, (-3) to 23 mmol m^{-2} yr^{-1} for phosphate and 0 to 1.2 mol m^{-2} yr^{-1} for silicate. These ranges are mainly attributable to large-scale variations over the whole area, even though there also exists a strong variability of fluxes between adjacent locations either sampled during one or more cruises. Most scatter in local data is observed in the "high-flux areas" off southwest Africa and Argentina (all GeoB-numbers that begin with 17 or 37 and 27 or 28 in Tables 2 and 4). We attribute these differences mainly to a high variability in the input of metabolizable/dissolvable material. In the central equatorial region it seems likely that seasonal effects are also reflected in the flux variance. In Figure 2, fluxes of locations between 25.5°-23°W and 1°S-2°N at water depths between 3700 and 4600 m (Table 2) are compared. Samples representing different seasons were collected in 1993, 1994, 1996, and 1987 [*Jahnke et al.*, 1989] respectively. The percentage deviation from the mean flux of the total data used in Figure 2 is 63% (nitrate), 95% (phosphate), and 60% (silicate). Mean percentage flux deviations for each month are much lower for nitrate (30%) and phosphate (67%), indicating that seasonal variations could add a substantial part of the total observed heterogeneity. The obviously contrasting dependency between nitrate and phosphate fluxes is unclear but could possibly be related to different qualities of decomposed OM. Unlike nitrate and phosphate, silicate fluxes do not seem to be subject to

seasonal variations as indicated by a similiar mean percentage flux deviation (57%) compared to the total percentage flux deviation.

4.2. Regionalization of Fluxes

Variogram analysis and kriging were carried out for nitrate, phosphate, and silicate fluxes. Histograms of data distributions (Figure 3) show that all parameters are more or less lognormally distributed. The geostatistical significance of whether a distribution is normal or lognormal is generally low, but it is more difficult to interpret variograms based on highly skewed distributions [*Englund and Sparks*, 1988]. For this reason, nitrate and silicate fluxes were transformed for variogram analysis. Phosphate data were not transformed since they include negative values. However, the extraction of negative phosphate values does not alter the model-variogram parameters (nugget, sill and range) significantly, so that the effect on the subsequent regionalization method can be neglected in case of phosphate fluxes. Variograms (Figure 3) suggest a regional dependency of the data which generally warrants the use of kriging. With a distance interval of 2.2°-2.5° a regional relation could be detected up to a range between 14° to 18°. Variogram results were fitted by spherical (nitrate and phosphate, Equation (4)) and exponential (silicate, Equation (5)) models:

spherical model

$$\gamma(h) = C \times \left(\frac{3}{2} \times \frac{|h|}{a} - \frac{|h|^3}{2 \times a^3} \right) \quad if\ |h| \le a \tag{4}$$

exponential model

$$\gamma(h) = C \times \left(1 - \exp\left[\frac{-|h|}{a} \right] \right) \tag{5}$$

where $\gamma(h)$ is the (semi) variogram, $|h|$ is the distance vector (increment), C is the sill value, and a is the range. Caused by the relatively clustered data-point distribution combined with a significant small-scale variability in these areas (e.g., high-flux areas; see also Table 4 and Figure 2), the nugget variances are comparatively high for each parameter, with the smallest "nuggets" for silicate. This effect occurs because of scatter of data, which cannot be resolved within the chosen length of the increment. The central equatorial region is a good example to show this effect. The range of data scatter is highest for phosphate and lowest for silicate (Figure 2), which is a fraction of the total observed nugget effect in Figure 3.

These deviations also become visible by comparing measured values and values estimated by the subsequent kriging procedure (Figure 4). Apart from a few outliers, observations and predictions agree within a factor of 2-3. However, owing to the smoothing effect inherent in the kriging procedure a better agreement is not truly expectable regarding the observed small-scale data scatter. Generally, the outliers or strong deviations of estimated values from measured values can be attributed to mainly two reasons: (1) A single measurement shows a result which is opposite to an areal trend, and (2) the variability of measurements is very high within a narrow cluster of locations (small-scale variabilty). In the first case the areal prediction would follow the general trend in this area, more or less ignoring the single outlier. In the second case the areal trend would be averaged over the total number of measurements considered. Although in both cases the single measurements will possibly deviate significantly from the estimates, the resulting estimate can be understood as a control of measured data instead of an error and supports the finding of a more uniform regional trend. Thus scattering is reduced by the kriging method providing smoothed data sets. The smoothing effect can be reduced by either using a smaller increment for the variogram analysis (downscaling) or by minimizing the number of points for an estimate within a certain range. Reducing the increment would, however, significantly affect the maximum range for data interpolation and therefore reduce the possibility of making predictions for large, sparsely sampled areas. Estimates in areas with very few data points over large distances actually have high variances, but this uncertainty is only of minor importance if there is a low variability of fluxes in these areas. The second possibility would result in better estimates for locations with adjacent data points but also lead to an overrating of isolated points and presumably creation of an unexplainable "statistical noise". Since the main objective is to

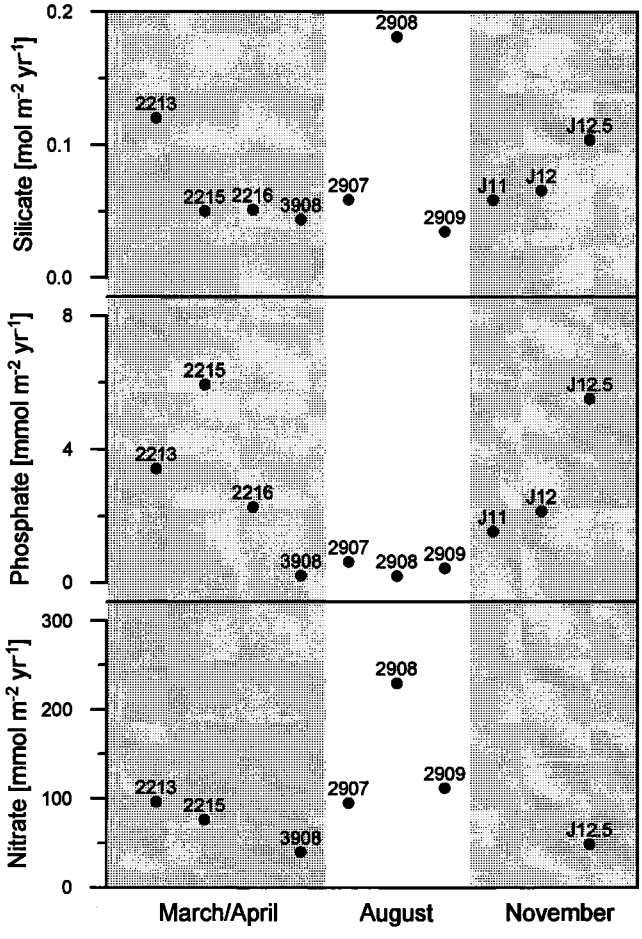

Figure 2. Seasonal variability of benthic fluxes in the central equatorial Atlantic. The sampling sites are situated between 25.5°-23°W and 1°S-2°N. Water depths range between 3700 and 4600 m. Despite a certain site to site variation for each parameter, there seems to be a seasonal pattern for nitrate and phosphate fluxes. The reason for the contrasting temporal release patterns of phosphate and nitrate is unknown but might be due to the different quality of decomposed OM.

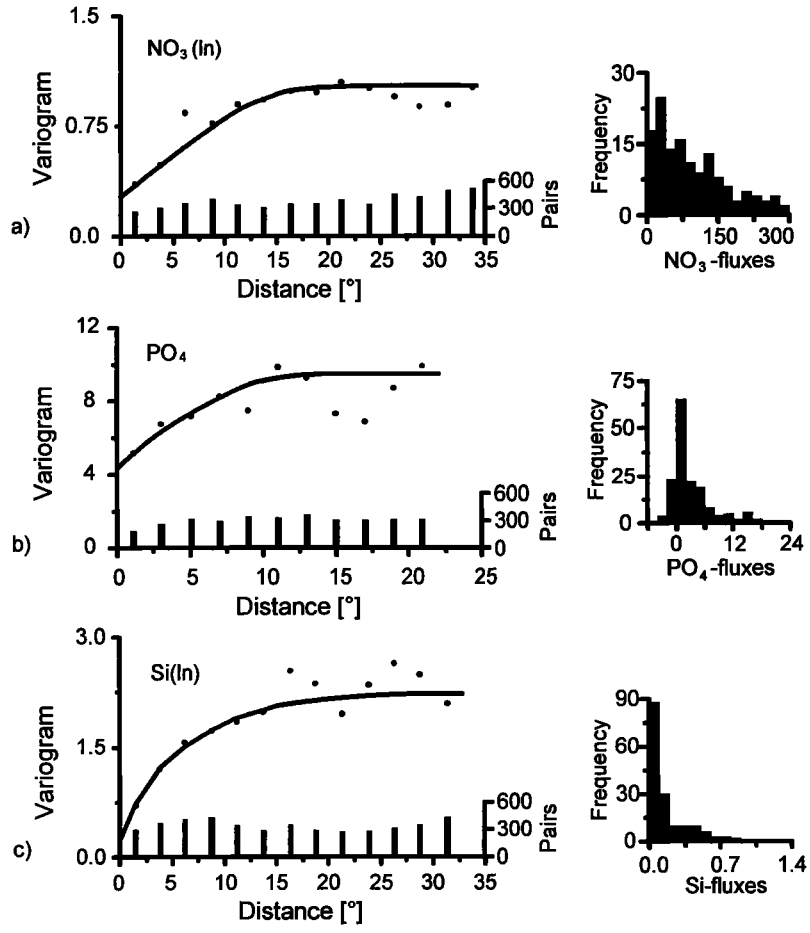

Figure 3. Experimental and model variograms of (a) nitrate, (b) phosphate, and (c) silicate flux variances. Experimental variograms are based on 2.4°, 2.2°, and 2.5° distance intervals for Figures 3a - 3c, respectively. The number of pairs underlying each variogram point within one distance interval is displayed on the second *y* axis. Parameters of model variograms are as follows: Figure 3a, spherical, nugget is 0.34, sill is 0.725, and range is 17°; Figure 3b, spherical, nugget is 4,5, sill is 5, and range is 14°; and Figure 3c, exponential, nugget is 0.35, sill is 1.8, and range is 18°. Model variograms, given through Equation (4) (Figures 3a and 3b) and Eqution (5) (Figure 3c), allow the conclusion of a regional dependency of the variables up to 14°-18°.

produce maps displaying the general distribution patterns of the investigated parameters over the total area, we accepted that existing site to site deviations (e.g., transects across the continental slope) were averaged out in order to extract the general trend.

4.3. Distribution Maps of Nitrate, Phosphate, and Silicate Fluxes

The resulting distribution maps of diffusive, benthic fluxes of nitrate, phosphate and silicate are presented in Plates 2-4. The continental margin area <1000 m water depth (pale blue color) is excluded from flux estimations. Data from areas < 1000 m were only considered in establishing the regional trend toward the coastal zone. The locations are displayed by different point sizes according to the measured fluxes. Areas with negative phosphate fluxes on Plate 3 are shown in the same color as fluxes below 0.25 mmol m^{-2} yr^{-1} to express their artificial origin.

Phosphate and silicate maps show some minor differences in the overlapping zones to the maps of *Zabel et al.* (1997) for the eastern South Atlantic. These differences result mainly from the coarser grid resolution and changes of kriging parameters because of the larger investigated area as well as the integration of additional data points used for this study.

The highest fluxes of all constituents are found in the regions off Southwest Africa and Argentina. The lowest fluxes occur within the central basin and Mid-Atlantic ridge area. Owing to the smoothing effect of the kriging method, extreme values were "filtered", resulting in reduced maximum ranges of the fluxes: nitrate, 10-180 mmol m^{-2} yr^{-1}; phosphate, (-2)-11 mmol m^{-2} yr^{-1}; and silicate, 0-0.65 mol m^{-2} yr^{-1}. The most striking feature of all maps is the relatively large area with high release rates extending into the western Argentine Basin. This is based on several sampling sites between 4400 and 5800 m (GeoB 2704, 2717, 2724, 2729, 2730, 2731, 2807, and 2808). Owing to the none-qual-area projection the areal extent appears proportionally enlarged at these latitudes compared to the remaining area. The opposite can be observed in the eastern Atlantic Ocean where the area of highest fluxes is more closely restricted to the continental slope. Obviously, the benthic flux pattern off southwest Africa fits well to the known relationships between PP and export of OM in dependency of water depth. In contrast, off Argentina,

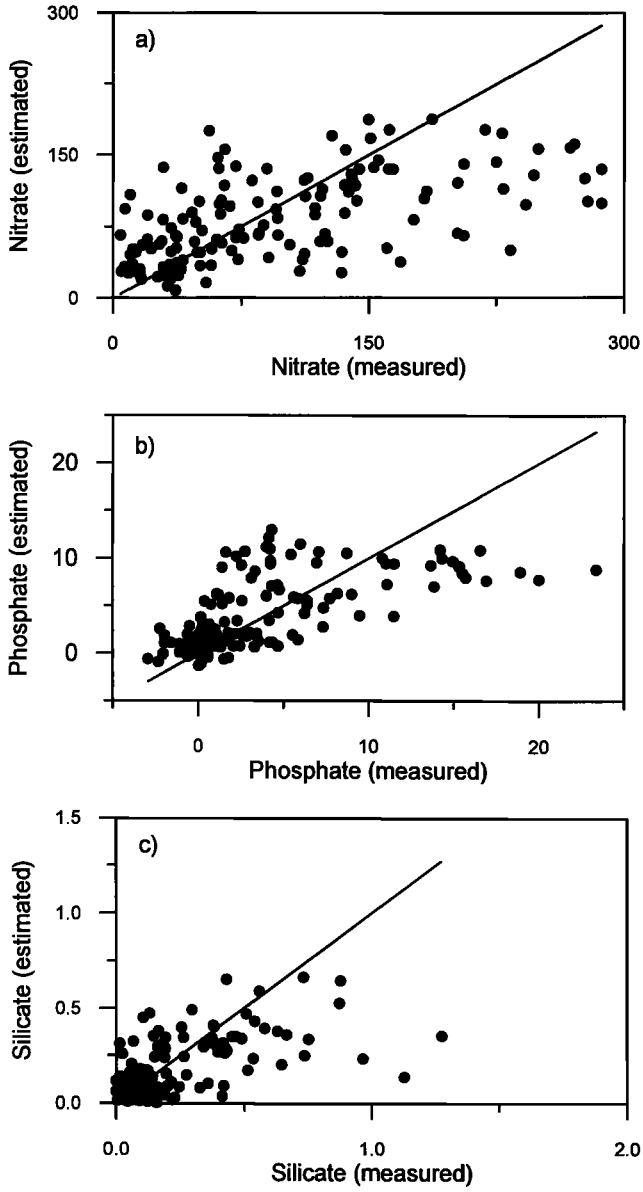

Figure 4. Comparison of calculated and estimated (kriged) benthic fluxes. Most estimations agree within a factor of 2-3. Outliers are due to the high variability of fluxes within closely sampled areas (see text for explanation). Fluxes are in mmol m^{-2} yr^{-1} (Figures 4a and 4b) and mol m^{-2} yr^{-1} (Figure 4c).

lateral transport processes and input of OM to deeper parts of the ocean seem to be more important [*Ledbetter and Klaus*, 1987], elevating mineralization and dissolution processes in the surface sediments on the lower continental slope and in the adjacent parts of the basin. The extent of the area of high benthic fluxes into the basin is probably overestimated because of the sparse sample density in the central Argentine Basin. The general trend, however, is conspicuous and partly supported by results of *Jahnke* [1996].

Global maps of primary productivity [*Berger et al.*, 1987; *Berger and Wefer*, 1991; *Antoine et al.*, 1996] display the most productive areas in the South Atlantic along the west African coast and the eastern equatorial region (Equatorial Divergence Zone). Elevated surface water productivity can also be detected for the Argentine shelf with a maximum in the Rio de la Plata region [*Antoine et al.*, 1996]. In the central basin and Mid-Atlantic ridge area and off the north Brazilian coast, production rates are lowest, apart from the Amazon River mouth.

Generally, there is some agreement of these patterns with our results. The most striking differences occur in the Guinea and the Northern Angola Basin, where high overall PP rates are reported by *Berger and Wefer* [1991] and *Antoine et al.* [1996]. These are not reflected by our maps. The reason for this discrepancy can be related to the sparse sampling in this region, especially along the continental margin. Owing to this the standard deviation of our estimated fluxes is reasonably high in these areas and gains importance in so far as we can expect an elevated benthic activity from the PP maps. In this case, additional measurements are required to control our estimates. Additionally, low benthic fluxes in this area could be related to a higher nutrient recycling in the surface waters, resulting in a lower export flux or a generally higher remineralization within the water column. Also, the differences between benthic fluxes in the western and eastern equatorial Atlantic, especially for nitrate and phosphate, are remarkable in this context. According to the PP maps, higher fluxes are to be expected in the eastern region. In contrast, our results display the reverse pattern, with higher fluxes in the western equatorial Atlantic. Since we have only measurements between February and April in the eastern equatorial Atlantic, this unexpected behavior could also be due to seasonal variabilty at least for nitrate and phosphate.

In the northwestern part of the study area the influence of the Amazon River on elevated PP [*DeMaster et al.*, 1996; *Antoine et al.*, 1996] is only weakly reflected by the benthic activity. We ascribe this finding to the fact that most of the OM is transported parallel to the coastline by the strong North Brazil Current [*Geyer et al.*, 1991] and is therefore not deposited farther offshore.

The benthic silicate fluxes in the Argentine Basin (Plate 4) reveal another very prominent pattern. Interestingly, this area of high silicate fluxes continues through the Vema Channel into the Brazil Basin. This pattern coincides with the flow path of the Antartic Bottom Water which enters the Argentine Basin east of the Falkland Plateau, flows as a contour current along the continental margin, and continues through the Vema Channel [*Emery and Uchupi*, 1984; *Ledbetter and Klaus*, 1987]. With the bottom water flow, biogenic sediments are transported over long distances [*Balsam and Wolhart*, 1993]. *Jones and Johnson* [1984] found that Antarctic diatoms are abundant in sediments below 4100 m water depth in the Vema Channel. Considering that Antarctic diatom frustules have a large dissolution rate [*van Bennekom et al.*, 1988], we conclude that the supply of Antarctic diatoms contributes significantly to benthic release of silicate in the Argentine Basin and the Vema Channel.

4.4 Quantification of Fluxes

Each distribution map is underlain by a 90×70 matrix with a homogenous 1° grid point resolution created by the kriging procedure and subsequent smoothing. Assuming that each estimate is representative for a 1°×1° area we calculated the total release of nitrate, phosphate, and silicate.

Total fluxes as well as average fluxes for the South Atlantic are given in Table 5. The total investigated area excluding the area <1000 m water depth off the coastline is about 32×10^6 km^2.

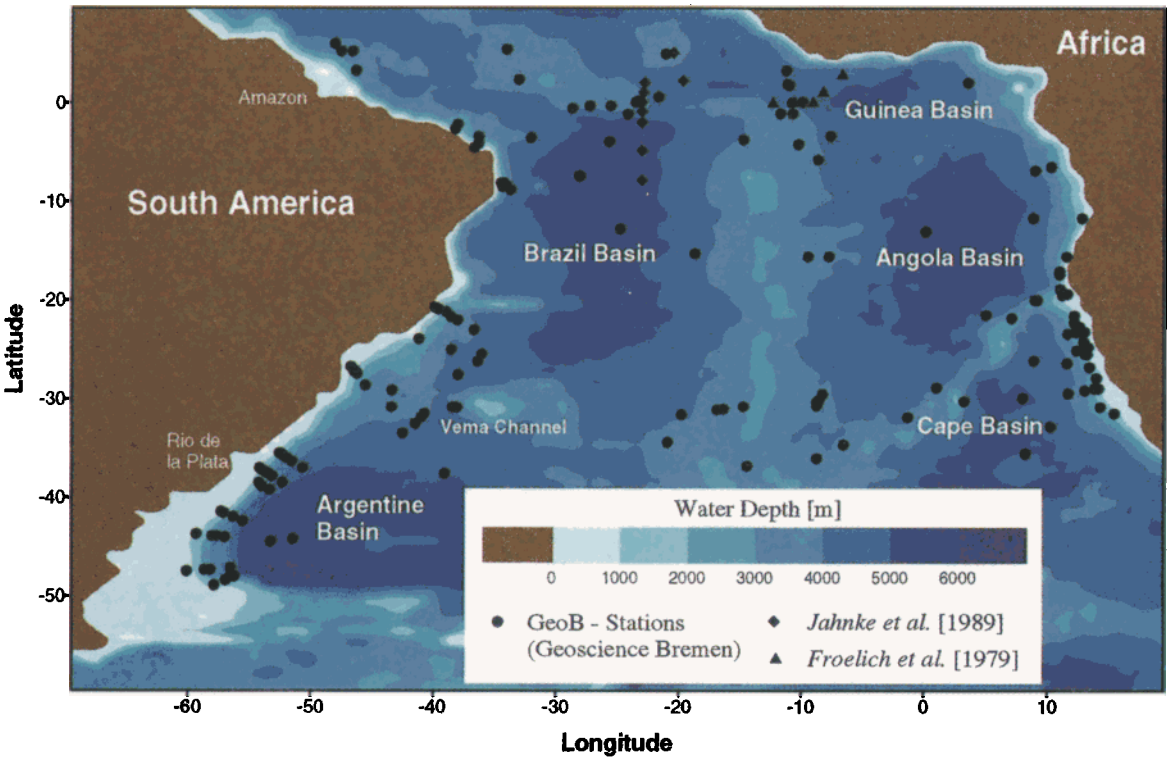

Plate 1. Sampling sites in the South Atlantic Ocean.

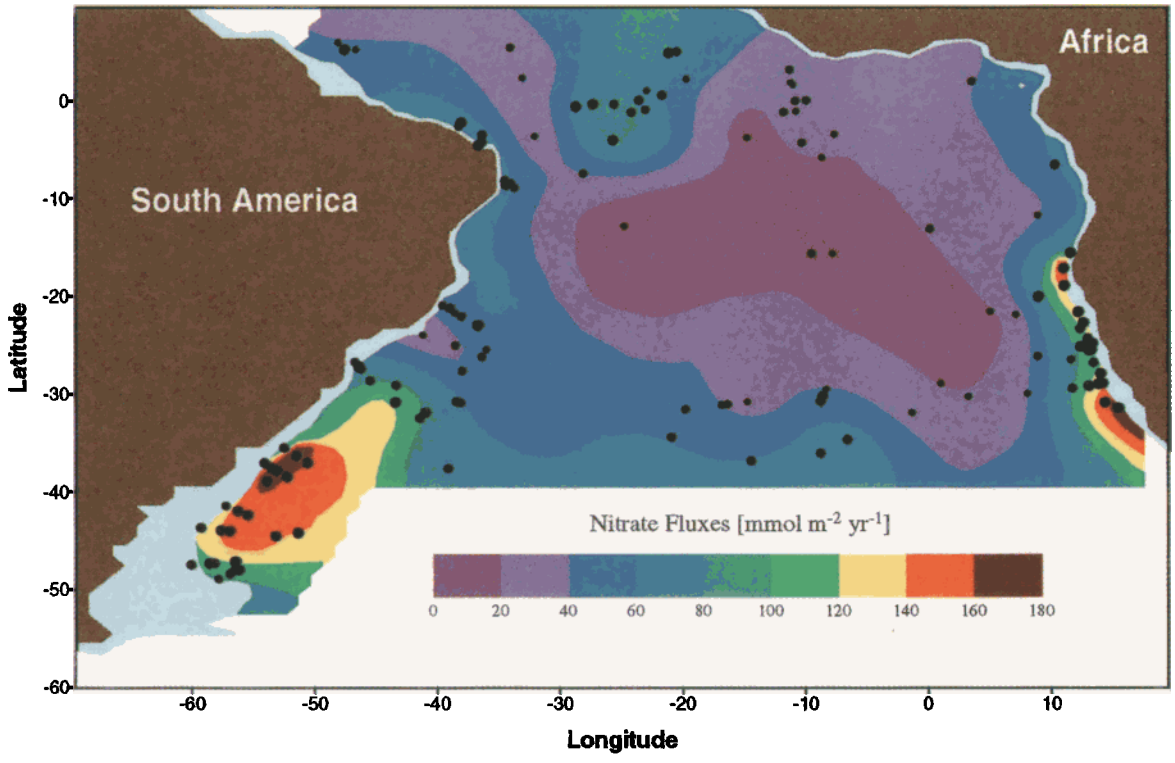

Plate 2. Regional distribution of benthic nitrate release rates. Locations are displayed with point sizes according to measured fluxes as follows: • 4-30, • 30-60, • 60-90, • 90-120, • 120-160, and • 160-280 mmol m^{-2} yr^{-1}, respectively

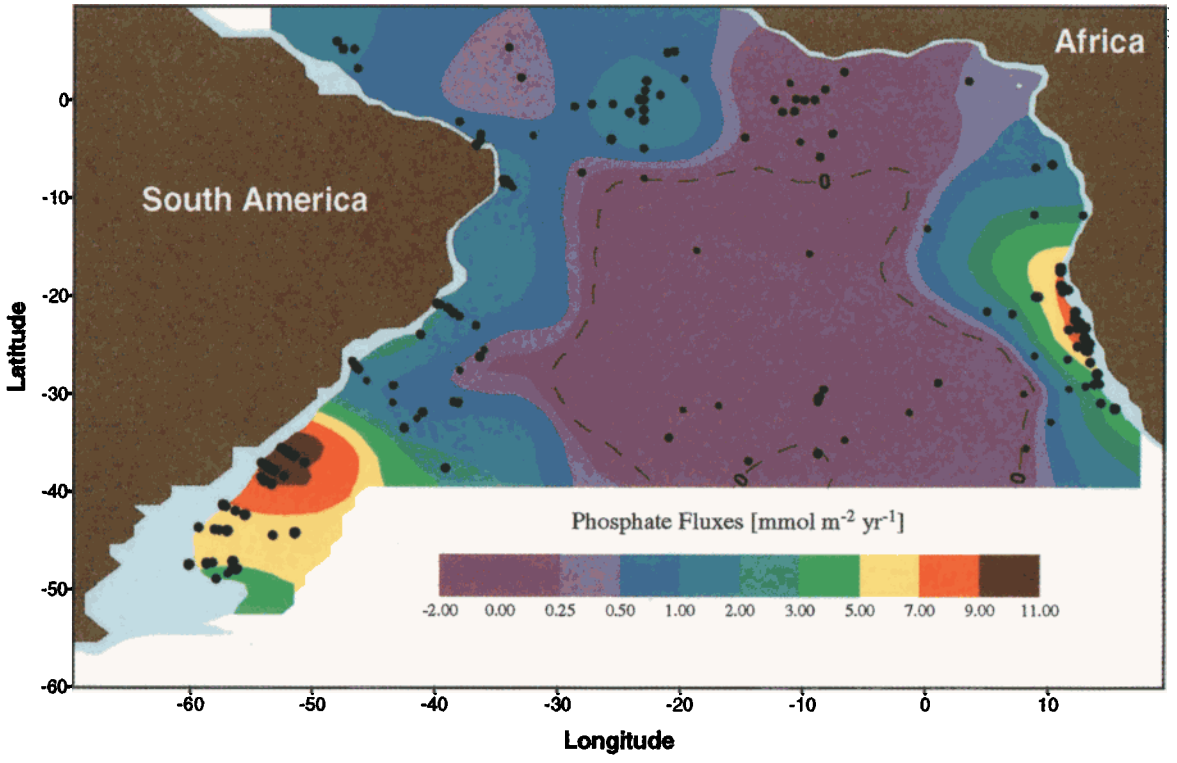

Plate 3. Regional distribution of benthic phosphate release rates. Locations are displayed with point sizes according to measured fluxes as follows: • (-3)-0, • 0-1, • 1-3, • 3-6, • 6-12, and • 12-20 mmol m^{-2} yr^{-1}, respectively.

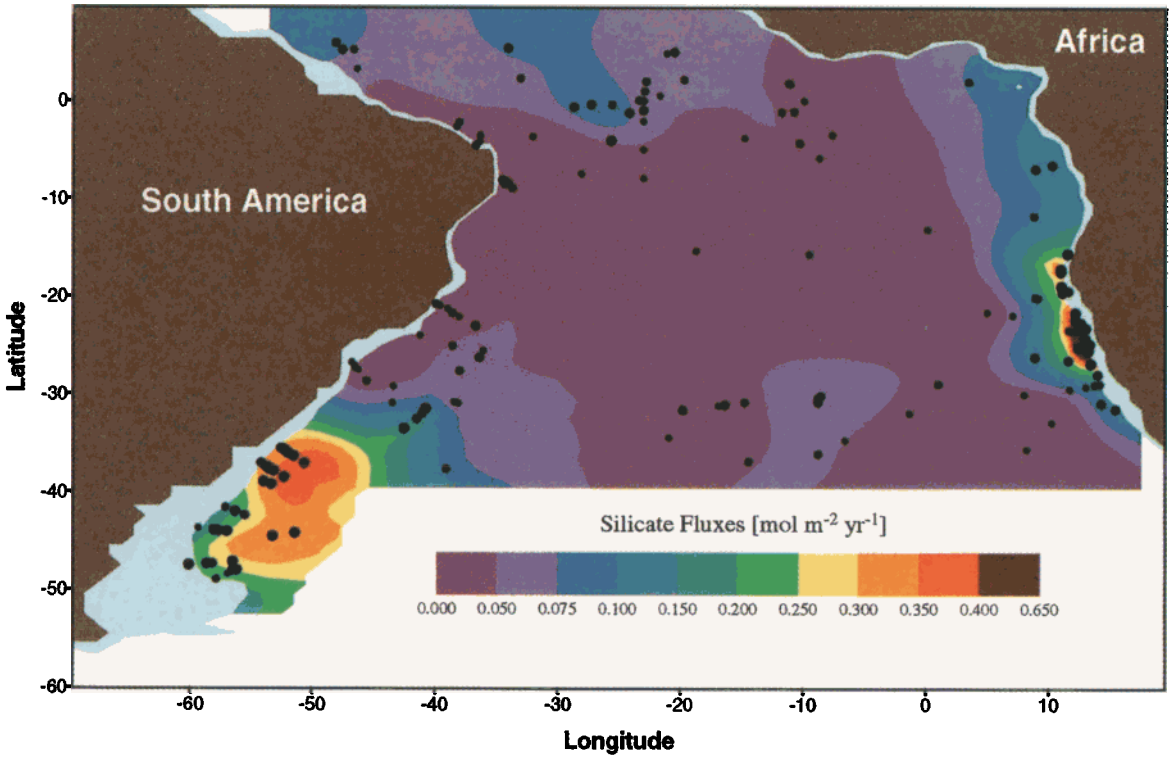

Plate 4. Regional distribution of benthic silicate release rates. Locations are displayed with point sizes according to measured fluxes as follows: • 0-0.05, • 0.05-0.1, • 0.1-0.15, • 0.15-0.25, • 0.25-0.45, and • 0.45-1.2 mmol m^{-2} yr^{-1}, respectively

Table 5. Total and Average Benthic Fluxes of Nitrate, Phosphate, and Silicate

	Benthic Fluxes (South Atlantic Ocean)			Benthic Fluxes (Global Projections)					
	Total,	Total Average,	Continental Margin Versus Open Ocean, [a]	This Study,	*Wollast* [1981], [b]	*Wollast* [1993], [b,c]	*Heath* [1974],	*Wollast and Mackenzie* [1983],	After *Mackenzie et al.* [1993], [b,c]
	mol yr^{-1}	mmol m^{-2} yr^{-1}	%	mol yr^{-1}	mol yr^{-1}	mol yr^{-1}	mol yr^{-1}	mol yr^{-1}	mol yr^{-1}
Nitrate	1.55×10^{12}	50	20 - 80	14.9×10^{12}	1.6×10^{12}	0.21×10^{12}	-	-	23×10^{12} (sedimentation-(burial plus denitrification))
Phosphate	3.5 (2.8-3.9) $\times10^{10}$, [d]	1.3, [d]	29 - 71 (± 4), [d]	31.8×10^{10}	4.2×10^{10}		-	-	81×10^{10} (sedimentation-burial)
Silicate	2.1×10^{12}	70	22 - 78	19.5×10^{12}	5.8×10^{12}		9.5×10^{12}	6.6×10^{12}	-

We estimated the percentages of total fluxes contributed by continental margin and open ocean sediments. The results of total fluxes are projected to the global ocean considering global areal proportions between continental margin and open ocean of 9.5% - 90.5 %. The global ocean area was estimated to be about 310×10^6 km^2 (without Arctic Ocean and continental margin area <1000 m water depth [*Kennett*, 1982]. Global estimates of benthic fluxes are compared to data of various authors. Dash indicates data not available.

[a] The area between 0-1000 m water depth is not included in the continental margin calculations. Relative areal proportions are 13.5% - 87.5%.

[b] Total release rates for N and P are given without considering species differentiation. We assume nitrate and phosphate as dominant species.

[c] Deep ocean only.

[d] Calculated under the assumption that phosphate fluxes are ≥ 0.25 mmol m^{-2} yr^{-1} at any location of the investigated area. Numbers in parenthesis refer to minimum fluxes of ≥ 0 and ≥ 0.5 mmol m^{-2}·yr^{-1}, respectively.

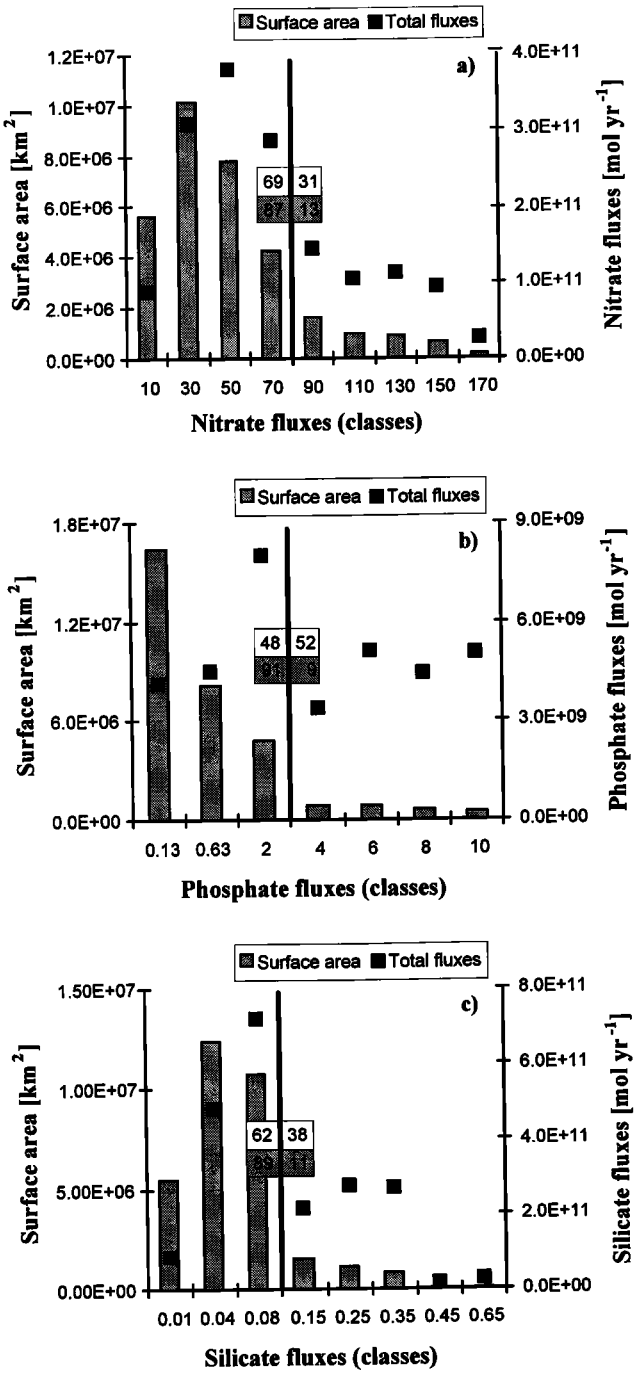

Figure 5. Histograms of benthic fluxes versus. seafloor area and total nutrient release. For each class the total flux is given for the corresponding seafloor area. The numbers in the box indicate the (top) proportions of total fluxes and (bottom) seafloor area between low and high fluxes (as indicated by the line). The relative importance of low-middle fluxes for the total release is pronounced especially for nitrate and silicate. This proportion is shifted for phosphate indicating the underestimation of phosphate fluxes due to recovery artifacts as discussed in the text.

About 13.5% of this area consists of continental margins (1000 to 4000 m water depth) which contribute about 20% of the total release of nitrate and silicate. This proportion underlines the relative importance of the open ocean, but a potential underestimation of fluxes on the continental margins (e.g., Guinea Basin and the Northern Angola Basin) must be considered. In contrast, phosphate release seems to be more important in continental margin areas (30% of the total). The estimation of phosphate fluxes, however, is subject to great uncertainties, considering that a large part of the central Atlantic shows negative fluxes. For the calculations of the total fluxes we assumed that phosphate fluxes are ≥ 0.25 mmol m^{-2} yr^{-1}, which marks the lower limit in Plate 3. Since we have no method to correct measured phosphate concentrations, we made this assumption to make fairly reasonable calculations. However, to give an estimation of uncertainty, we varied the arbitrary chosen lower limit between ≥ 0 and ≥ 0.5 (Table 5), indicating a variability of total phosphate fluxes by up to 20%. The effects on the proportional contribution of continental margin and open ocean are insignificant. The calculations of the total phosphate flux should, in any case, be understood as a minimum estimate.

As a further data analysis we present histograms of benthic nutrient fluxes versus seafloor area and total nutrient release in Figure 5. The areal proportions between low-middle and high fluxes are similiar for all nutrients (about 89↔11%). The limit between high and low fluxes was defined by the sharpest break of areal and total flux contribution within the flux classes in question (as indicated by the lines in Figure 5). The histograms underline the relative importance of low-middle flux rates for the total benthic nutrient release by indicating that about two thirds of the total fluxes of nitrate and silicate are contributed by the lower classes. For phosphate a proportion of about 1:1 is calculated, suggesting that high-flux areas are more important. However, assuming that a similiar pattern to those of nitrate and silicate between the areal and total flux contribution is more realistic, this result might again indicate an underestimation of phosphate fluxes which has more effect on the total contribution of the low fluxes because of their higher areal proportion.

Over the total area we calculated average release rates of nitrate and phosphate with a ratio of 35/1 (N/P). Compared to the Redfield N/P ratio of decomposed OM, which is generally assumed to be about 16/1, the difference is more than a factor of 2. This big difference can be attributed to the sampling artifacts discussed (underestimation of phosphate and overestimation of nitrate fluxes). However, an increased N/P ratio should be expected anyway since naturally occurring phosphate adsorption on mineral surfaces is a common process in marine sediments (assuming that denitrification is of minor importance in open ocean settings). Average silicate fluxes are about 0.07 mol m^{-2} yr^{-1}, which is about 1 order of magnitude more than estimated by *Wollast and Mackenzie* [1983] for the South Atlantic.

Assuming the South Atlantic to be representative for the world ocean (without the Arctic Ocean), we give estimations for the global benthic release rates of nitrate, phosphate, and silicate (Table 5). As above, we excluded the continental margin area < 1000 m from our calculations and considered the different areal proportion between continental margin and open ocean on a global scale.

Because the flux patterns derived for the South Atlantic do not necessarily correspond to the world ocean situation, these calculations should be understood as rough estimates. However, global benthic release rates of silicate come up to be a factor of 2-3 higher than previous estimates made by *Heath* [1974], *Wollast* [1981] and *Wollast and Mackenzie* [1983]. Generally, the esti-

Table 6. Global Estimations of River Input of Dissolved Nitrogen, Phosphorus, and Silicate

	Mackenzie et al. [1993] [a]	*After Meybeck* [1993] [b]	*Heath* [1974]	*Wollast & Mackenzie* [1983]
Nitrogen	$1.03 \cdot 10^{12}$	$3 \cdot 10^{11}$	-	-
Phosphorus	$3 \cdot 10^{10}$	$1.2 \cdot 10^{10}$	-	-
Silicate	-	-	$7.2 \cdot 10^{12}$	$7.25 \cdot 10^{12}$

Values are in units of mol yr^{-1}. Dash indicates data not available.
[a] Including dissolved organic N and P species.
[b] Values are based on a global river discharge of 37,400 km^3 yr^{-1} [*Wollast and Mackenzie*, 1983].

mates presented by these authors are based on the assumption of linear concentration gradients over several centimeters, which leads to underestimations considering the asymptotic shape of silicate concentration profiles close to the sediment-water interface. Consequently, our estimates of benthic silicate release exceed the input of dissolved silicate by rivers by about a factor of 3 (Table 6). *DeMaster* [1979]; cited by *Kennett*, 1982] already claimed that the release from interstitial water in deep-sea sediments is greater than the global input from rivers. This is confirmed by our results if the estimates for the global river input are not significantly underestimated. Furthermore, our estimates reveal that benthic release accounts for about 4-6% of the maximum annual Si production of 280 to $500 \cdot 10^{12}$ mol [*Wollast*, 1981; *Calvert*, 1983; *Nelson et al.*, 1995], emphasizing the relative importance of the benthic release of silicate in the global oceanic Si cycle.

A comparison of our global nitrate and phosphate fluxes with results presented in other publications is more difficult, since fluxes of different inorganic N and P species as well as dissolved organic N and P are often summed up. Nitrate is the most stable fixed nitrogen compound in oxygenated waters. Therefore the nitrate release might be comparable in magnitude to the total release of inorganic nitrogen compounds in the deep ocean. The proportion of dissolved organic compounds, however, remains difficult to assess. The estimations of *Wollast* [1981] for the global ocean release and the global deep ocean release [*Wollast*, 1993] of N and P are about 1-2 orders of magnitude lower than our estimates. In contrast, calculations for deep ocean sediments by *Mackenzie et al.* [1993], which include organic compounds, are 46% (N) and 39% (P) higher than ours (Table 5). These discrepancies illustrate the need for more detailed investigations to quantify benthic reflux in the global nutrient cycle. Our results, however, reveal that benthic fluxes of *Wollast* [1981, 1993] seem to be underestimated, since they are significantly lower than or nearly equal to our calculations of open ocean fluxes for the South Atlantic only. However, benthic fluxes of nitrate and phosphate seem to be far more important than dissolved nitrogen and phosphorus input by rivers (Table 6).

Jahnke [1996] estimated a total deep ocean oxygen utilization of 1.2×10^{14} mol yr^{-1} (≥ 1000 m water depth). He further concluded that 45% of the deep ocean OM remineralization occurs in the sediments. Assuming that oxygen consumption in deep ocean sediments is exclusively driven by OM remineralization and a reaction stoichiometry of 106/16/1/138 ($C/N/P/O_2$), we calculated the corresponding release of nitrate and phosphate. If denitrification and adsorption of phosphate are neglected, benthic nitrate release is about a factor of 2.5 lower and phosphate release about a factor of 2 higher than our estimates given in Table 5. The estimation from oxygen data is, of course, a very rough estimate with significant errors due to denitrification on continental margins, preferential degradation of nitrogen-rich OM, and adsorption/precipitation processes, but it is in agreement with our assumption of an underestimation of phophate fluxes and overestimation of nitrate fluxes. Overall, however, our estimations are of the same order of magnitude as those derived by other authors.

Assuming our estimates are correct, nitrate and phosphate reflux from deep ocean sediments account for about 3-4% and 1%, respectively, of annual global ocean PP ($2.5\text{-}3.3 \times 10^{15}$ mol C) [*de Baar and Suess*, 1993; *Antoine et al.*, 1996] assuming Redfield composition of OM.

5. Concluding Remarks

In our study we present an approximation of benthic release rates of nitrate, phosphate, and silicate for the South Atlantic Ocean and projections for the global deep ocean area. Even if we have to account for some restrictions of data interpolation for certain areas, for example very low fluxes on the continental slope of the Guinea Basin and the Northern Angola Basin, and sampling artifacts, the resulting overall pattern provides a good measure for the magnitude of the investigated parameters. This is verified by the reasonably good agreement of our estimates with those derived from literature on a global scale. Furthermore, the analysis of the extensive data sets revealed interesting regional trends different from compilations of primary production in surface waters (e.g., Argentine Basin and Northern Angola / Guinea Basins) indicating regional inhomogeneities in supply mechanisms controlling the input of OM and biogenic silica to the seafloor. Our results emphasize the importance of deep ocean sediments for the reflux of nutrients into the bottom water and therefore for the nutrient and carbon cycle in the world ocean. However, we are aware of the fact that global-scale variability in release rates might be even more pronounced than observed in the South Atlantic. Since it is difficult to produce a comparable data set for the world ocean, it will be necessary to derive benthic fluxes from more easily accessible parameters (e.g., satellite data). In this context further investigations on the relationships between OM supply to the sediment, reaction stoichiometry, and benthic release of nutrients are required. Our estimates, however, might be suitable to evaluate future predictions of benthic nutrient fluxes.

Acknowledgments. We would like to thank W.H. Berger, R. Haese, S. Kasten, and J. Schröter for their valuable criticism during the development of the manuscript. We greatly appreciate the very helpful and constructive reviews of D. Burdige, D. Hammond, and an anonymous reviewer. Porosity data of Meteor cruises M6, M9, M16, and M20 were kindly provided by P.J. Müller. This research was funded by the Bundesministerium für Bildung, Wissenschaft, Forschung und Technologie within the framework of the German JGOFS Program and the Deutsche Forschungsgemeinschaft (Sonderforschungsbereich 261 at Bremen University, Contribution 170).

References

Akin, H., and H. Siemes, *Praktische Geostatistik*, Springer-Verlag, Berlin-Heidelberg, 1988.

Aller, R.C., Benthic fauna and biogeochemical processes in marine sediments: The role of burrow structures, in *Nitrogen Cycling in Coastal Marine Environments*, edited by T.H. Blackburn and J. Sørensen, pp. 301-338, John Wiley, New York, 1988.

Antoine, D., J.-M. André, and A. Morel, Oceanic primary production, 2., Estimation at global scale from satellite (coastal zone color scanner) chlorophyll, *Global Biogeochem. Cycles, 10*, 57-69, 1996.

Archer, D., and A. Devol, Benthic oxygen fluxes on the Washington shelf and slope: A comparison of in situ microelectrode and chamber flux measurements, *Limnol. Oceanogr., 37*, 614-629, 1992.

Archer, D., M. Lyle, K. Rodgers, and P. Froelich,. What controls opal preservation in tropical deep-sea sediments?, *Paleoceanography, 8*(1), 7-21, 1993.

Bainbridge, A.E., *GEOSECS - Atlantic Expedition*, vol. 2, *Sections and profiles*, National Science Foundation,Washington D.C., 1976.

Balsam, W.L., and R.J. Wolhart, Sediment dispersal in the Argentine Basin: Evidence from visible light spectra, *Deep Sea Res., Part II, 40*, 1001-1031, 1993.

Berelson, W.M., D.E. Hammond, D. O'Neill, X.-M. Xu, C. Chin, and J. Zukin, Benthic fluxes and pore water studies from sediments of the central equatorial north Pacific: Nutrient diagenesis, *Geochim. Cosmochim. Acta, 54*, 3001-3012, 1990.

Berger, W.H., Appendix global maps of ocean productivity, in *Productivity of the Ocean: Present and Past*, edited by W.H. Berger et al., pp. 429-455, John Wiley, New York, 1989.

Berger, W.H., and G. Wefer, Productivity of the glacial ocean: Discussion of the iron hypothesis, *Limnol. Oceanogr., 36*, 1899-1918, 1991.

Berger, W.H., K. Fischer, C. Lai, and C. Wu, Ocean productivity and organic carbon flux. I. Overview and maps of primary production and export production, *SIO Ref. 87-30*, Univ. of Calif., San Diego, 1987.

Berger, W.H., V. Smetacek, and G. Wefer, Ocean productivity and paleoproductivity - An overview, in *Productivity of the Ocean: Present and Past*, edited by W.H. Berger et al., pp. 1-34, John Wiley, New York, 1989.

Betzer, P.R., W.J. Showers, E.A. Laws, C.D. Winn, G.R. Di Tullio, and P.M. Kroopnick, Primary productivity and particle fluxes on a transect of the equator at 153 W in the Pacific, *Deep Sea Res., Part. A, 31*, 1-11, 1984.

Calvert, S.E., Sedimentary geochemistry of silicon, in *Silicon Geochemistry and Biogeochemistry*, edited by S.R. Aston, pp. 143-186, Academic, San Diego, Calif., 1983.

Canfield, D.E., Organic matter oxidation in marine sediments, in *Interactions of C, N, P, and S in Biogeochemical Cycles*, edited by R. Wollast et al., *NATO ASI Ser., Ser. I, 4*, 333-363, 1993.

Davis, J.C., *Statistics and data analysis in geology*, John Wiley, New York, 1986.

de Baar, J.W., and E. Suess, Ocean carbon cycle and climate change - An introduction to the Interdisciplinary Union Symposium, *Global Planet. Change, 8*, VII-XI, 1993.

DeMaster, D.J., The marine budgets of Silica and ^{32}Si, Ph.D. dissertation, New Haven, Conn., Yale Univ., 1979.

DeMaster, D.J., W.O. Smith Jr., D.M. Nelson, and J.Y. Aller, Biogeochemical processes in Amazon shelf waters: Chemical distributions and uptake rates of silicon, carbon and nitrogen, *Cont. Shelf Res., 16*, 617-643, 1996.

Emerson, S., and J.I. Hedges, Processes controlling the organic carbon content of open ocean sediments, *Paleoceanography, 3*(5), pp. 621-634, 1988.

Emery, W.J., and E. Uchupi, *The Geology of the Atlantic Ocean*, Springer Verlag, New York, 1984.

Englund, E., and A. Sparks, GEO-EAS (Geostatistical Environmental Assesment Software) User's Guide, *Rep. 600/4-88/033a*, U.S. Environmental Protection Agency, Las Vegas, Nev., 1988.

Froelich, P.N., G.P. Klinkhammer, M.L. Bender, N.A. Luedtke, G.R. Heath, D. Cullen, P. Dauphin, D. Hammond, B. Hartman, and V. Maynard, Early oxidation of organic matter in pelagic sediments of the eastern equatorial Atlantic: Suboxic diagenesis, *Geochim. Cosmochim. Acta, 43*, 1075-1090, 1979.

Geyer, W.R., R.C. Beardsley, J. Candela, B.M. Castro, R.V. Legeckis, S.J. Lentz, R. Limeburner, L.B. Miranda, and J.H. Trowbridge, The physical oceanography of the Amazon outflow, *Oceanography, 4*, 8-14, 1991.

Glud, R.N., J.K. Gundersen, B.B. Jørgensen, N.P. Revsbech, and H.D. Schulz, Diffusive and total uptake of deep-sea sediments in the eastern South Atlantic Ocean: In situ and laboratory measurements, *Deep Sea Res., 41, Part I*, 1767-1788, 1994.

Grasshoff, K., M. Ehrhardt, and K. Kremling, *Methods of Seawater Analysis*, Verlag Chemie, Weinheim, Germany, 1983.

Hammond D. E., J. McManus, W. M. Berelson, T .E. Kilgore, and R. H. Pope: Early diagenesis of organic material in equatorial Pacific sediments: Stoichiometry and kinetics.- *Deep Sea Research, Part II, 43*, 1365-1412, 1996.

Heath, G.R., Dissolved silica and deep-sea sediments, in *Studies in Paleoceanography*, edited by W.W. Hay, *Spec. Publ. Soc. Econ. Paleontol. Mineral., 20*, 77-93, 1974.

Henrichs, S.M., and W.S. Reeburgh, Anaerobic mineralization of marine sediment organic matter: Rates and the role of anaerobic processes in the oceanic carbon economy, *J. Geomicrobiol., 5*, 191-237, 1987.

Hensen, C., H. Landenberger, M. Zabel, J. Gundersen, R.N. Glud, and H.D. Schulz, Simulation of early diagenetic processes in continental slope sediments off southwest Africa: The Computer model CoTAM tested, *Mar. Geol.*, in press, 1997.

Jahnke, R.A., The global ocean flux of particulate organic carbon: Areal distribution and magnitude, *Global Biogeochem. Cycles, 10*, 71-88, 1996.

Jahnke, R.A., and G.A. Jackson, Role of sea floor organisms in oxygen consumption in the deep North Pacific Ocean, *Nature, 329*, 621-623, 1987.

Jahnke, R.A., D. Heggie, S. Emerson, and V. Grundmanis, Pore waters of the central Pacific Ocean: Nutrient results, *Earth Planet. Sci. Lett., 61*, 233-256, 1982a.

Jahnke, R.A., S.R. Emerson, and J.W. Murray, A model of oxygen reduction, denitrification, and organic matter mineralization in marine sediments, *Limnol. Oceanogr., 27*, 610-623, 1982b.

Jahnke, R.A., S.R. Emerson, C.E. Reimers, J. Schuffert, K. Ruttenberg, and D. Archer, Benthic recycling of biogenic debris in the eastern tropical Atlantic ocean, *Geochim. Cosmochim. Acta, 53*, 2947-2960, 1989.

Jahnke, R.A., C.E. Reimers, and D.B. Craven, Intensification of recycling of organic matter at the sea floor near ocaen margins, *Nature, 348*, 50-54, 1990.

Jones, G.A., and D.A. Johnson, Displaced antarctic diatoms in Vema Channel sediments: Late Pleistocene/Holocene fluctuations in AABW flow, *Mar. Geol., 58*, 165-186, 1984.

Kennett, J.P., *Marine Geology*, Prentice-Hall Inc., Englewood Cliffs, N. J., 1982.

Ledbetter, M.T., and A. Klaus, Influence of bottom currents on sediment texture and sea-floor morphology in the Argentine Basin, in *Geology and Geochemistry of Abyssal Plains*, edited by P.P.E. Weaver and J. Thomson, *Geol. Soc. Spec. Publ., 31*, 23-31, 1987.

Lerman, A., *Geochemical Processes in Water and Sediment Environments*, John Wiley, New York, 1979.

Li, Y.-H., and S. Gregory, Diffusion of ions in sea water in deep-sea sediments, *Geochim. Cosmochim. Acta, 38*, 703-714, 1974.

Mackenzie, F.T., L.M. Ver, C. Sabine, M. Lane, and A. Lerman, C, N, P, S global biogeochemical cycles and modeling of global change, in *Interactions of C, N, P and S Biogeochemical Cycles and Global Change*, edited by R. Wollast et al., *NATO ASI Ser., Ser. I, 4*, 1-61, 1993.

Meybeck, M., C, N, P and S in rivers: From sources to inputs, in *Interactions of C, N, P and S Biogeochemical Cycles and Global Change*, edited by R. Wollast et al., *NATO ASI Ser., Ser. I, 4*, 163-193, 1993.

Nelson, D.M., P. Tréguer, M.A. Brzezinski, A. Leynaert, and B. Quéguiner, Production and dissolution of biogenic silica in the ocean: Revised global estimates, comparison with regional data and relationship in biogenic sedimentation, *Global Biogeochem. Cycles, 9*, 359-372, 1995.

Rowe, G.T., G.S. Boland, W.C. Phoel, R.F. Anderson, and P.E. Biscaye, Deep-sea floor respiration as an indication of lateral input of biogenic detritus from continental margins, *Deep Sea Res., Part II, 41*, 657-668, 1994.

Rutgers van der Loeff, M.M., and A.J. van Bennekom, Weddell Sea contributes little to silicate enrichment in Antarctic Bottom Water, *Deep Sea Res., Part A, 36*, 1341-1357, 1989.

Sayles, F.L., and W.R. Martin, In situ tracer studies of solute transport across the sediment-water interface at the Bermuda Time Series site, *Deep Sea Res., Part I, 42*, 31-52, 1995.

Sayles, F.L., W.R. Martin, and W.G. Deuser, Response of benthic oxygen demand to particulate organic carbon supply in the sea near Bermuda, *Nature, 371*, 686-689, 1994.

Sayles, F.L., W.G. Deuser, J.E. Goudreau, W.H. Dickinson, T.D. Jickells, and P. King, The benthic cycle of biogenic opal at the Bermuda Atlantic Time Series site, *Deep Sea Res., Part I, 43*, 383-409, 1996.

Schulz, H.D., A. Dahmke, U. Schinzel, K. Wallmann, and M. Zabel, Early diagenetic processes, fluxes, and reaction rates in sediments of the South Atlantic, *Geochim. Cosmochim. Acta, 58*, 2041-2060, 1994.

Smith, K.L., Jr., and R.J. Baldwin, Seasonal fluctuations in deep-sea sediment community oxygen consumption: Central and eastern North Pacific, *Nature, 307*, 624-626, 1984.

Suess, E., Particulate organic carbon flux in the ocean-surface productivity and oxygen utilization, *Nature, 288*, 260-263, 1980.

Swan, A.R.H., and M. Sandilands, *Introduction to Geological Data Analysis*, Blackwell Sci., Cambridge, Mass., 1995.

Ullman, W.J., and R.C. Aller, Diffusion coefficients in nearshore marine sediments, *Limnol. and Oceanogr., 27*, 552-556, 1982.

van Bennekom, A.J., G.W. Berger, S.J. van der Gaast, and R.T.P. de Vries, Primary productivity and the silica cycle in the Southern Ocean (Atlantic Sector), *Palaeogeogr. Palaeoclimatol. Palaeoecol., 67*, 19-30, 1988.

Wollast, R., Interactions between major biogeochemical cycles in marine environments, in *Some perspectives of the Major Biogeochemical Cycles*, edited by G.E. Likens, *SCOPE, 17*, 125-142, 1981.

Wollast, R., Interactions of carbon and nitrogen cycles in the coastal zone, in *Interactions of C, N, P and S Biogeochemical Cycles and Global Change*, edited by R. Wollast et al., *NATO ASI Ser., Ser. I, 4*, 195-210, 1993.

Wollast, R., and F.T. Mackenzie, The global cycle of silica, in *Silicon Geochemistry and Biogeochemistry*, edited by S.R. Aston, pp. 39-76, Academic, San Diego, Calif., 1983.

Zabel, M., A. Dahmke, and H.D. Schulz, Regional distribution of diffusive phosphate and silicate fluxes through the sediment water interface - The eastern South Atlantic, *Deep Sea. Res, Part I*, in press, 1997.

C. Hensen, H. Landenberger, H.D. Schulz, and M. Zabel, Fachbereich Geowissenschaften, Universität Bremen, Postfach 330 440, 28334 Bremen, Germany. (e-mail: hensen@geochemie.uni-bremen.de; hland@geochemie.uni-bremen.de; hdschulz@geochemie.uni-bremen.de; mzabel@geochemie.uni-bremen.de)

(Received November 18, 1996; revised September 10, 1997; accepted September 18, 1997)